ISSN 1069-3513, Izvestiya, Physics of the Solid Earth, 2007, Vol. 43, No. 7, pp. 559–572. © Pleiades Publishing, Ltd., 2007.
Original Russian Text © V.I. Ulomov, T.I. Danilova, N.S. Medvedeva, T.P. Polyakova, L.S. Shumilina, 2007, published in Fizika Zemli, 2007, No. 7, pp. 31–45.

Assessment of Seismic Hazard in the North Caucasus

V. I. Ulomov, T. I. Danilova, N. S. Medvedeva, T. P. Polyakova, and L. S. Shumilina†

Schmidt Institute of Physics of the Earth (IPE), Russian Academy of Sciences (RAS),
Bol'shaya Gruzinskaya ul. 10, Moscow, 123995 Russia
e-mail: ulomov@ifz.ru

Received October 3, 2006

Abstract—The seismicity of the North Caucasus is the highest in the European part of Russia. The detection of potential seismic sources here and long-term prediction of earthquakes are extremely important for the assessment of seismic hazard and seismic risk in this densely populated and industrially developed region of the country. The seismogenic structures of the Iran–Caucasus–Anatolia and Central Asia regions, adjacent to European Russia, are the subjects of this study. These structures are responsible for the specific features of regional seismicity and for the geodynamic interaction with adjacent areas of the Scythian and Turan platforms. The most probable potential sources of earthquakes with magnitudes $M = 7.0 \pm 0.2$ and 7.5 ± 0.2 in the North Caucasus are located. The possible macroseismic effect of one of them is assessed.

PACS numbers: 91.30.Px

DOI: 10.1134/S1069351307070051

INTRODUCTION

The North Caucasus is characterized by the highest seismic activity in European Russia. In the seismogeodynamic respect, it belongs to the Iran–Caucasus–Anatolia region, in which very large earthquakes are inherent. The detection of potential earthquake sources (PESs) in the North Caucasus and long-term prediction of their activation are of paramount importance for adequate assessment of seismic hazard and seismic risk in this densely populated and industrially developed region of the country.

As was shown in [Ulomov et al., 2006], the Iran–Caucasus–Anatolia and Central Asia regions, together with transition zones between the mountainous structures and the Scythian and Turan platforms, form a coherent seismogeodynamic system responsible for the specific features of the seismic regime of this vast territory. Investigations of the spatial–temporal and energy development of seismogeodynamic processes along the main seismogenerating structures have revealed regular patterns in the sequence of seismic events with various magnitudes and in the migration of seismic activation.

The study described in this paper is intended to reveal potential sources of strong earthquakes in the North Caucasus and Ciscaucasia and is based on new ideas of the seismogeodynamics of seismically active regions and the spatial–temporal and energy ordering of their seismogenerating structures; these ideas were first developed for Central Asia [Ulomov, 1974] and were later elaborated in studies on the seismic zoning of North Eurasia and in the development of methods for long-term prediction of seismic danger [Ulomov, 1999; Ulomov and Shumilina, 1999].

The term "seismogeodynamics," proposed by V.I. Ulomov in the mid-1960s, has been extensively used in seismological practice (in our country and abroad) since the 1970s. As distinct from seismotectonics, which predominantly studies the static and geometric relations between seismic sources and tectonics, seismogeodynamics is concerned with the nature of seismicity as a result of motion of the crust and the entire lithosphere, taking into account their deep structure, strength properties, hierarchic fault–block structure, stress–strain state, and fracture processes at different scale levels (from local sources of individual earthquakes to regional and global seismogenerating structures). However, the key role belongs to the spatial–temporal development of seismic activation (deformation waves, earthquake source migration, etc.).

Along with the seismogeodynamic reconstructions performed for Central Asia in [Ulomov, 1974], similar investigations in the Iran–Caucasus–Anatolia region and the zone of its contact with the Scythian platform are the main subject of this work.

SEISMIC CONDITIONS IN SOUTHERN EUROPEAN RUSSIA

The North Caucasus is a part of the extended Crimea–Caucasus–Kopet Dagh zone of the seismically active Iran–Caucasus–Anatolia region and is characterized by a high seismic activity. Figure 1 shows the map of source seismicity and fragments of the normative maps of general seismic zoning of the Russian Federa-

† Deceased.

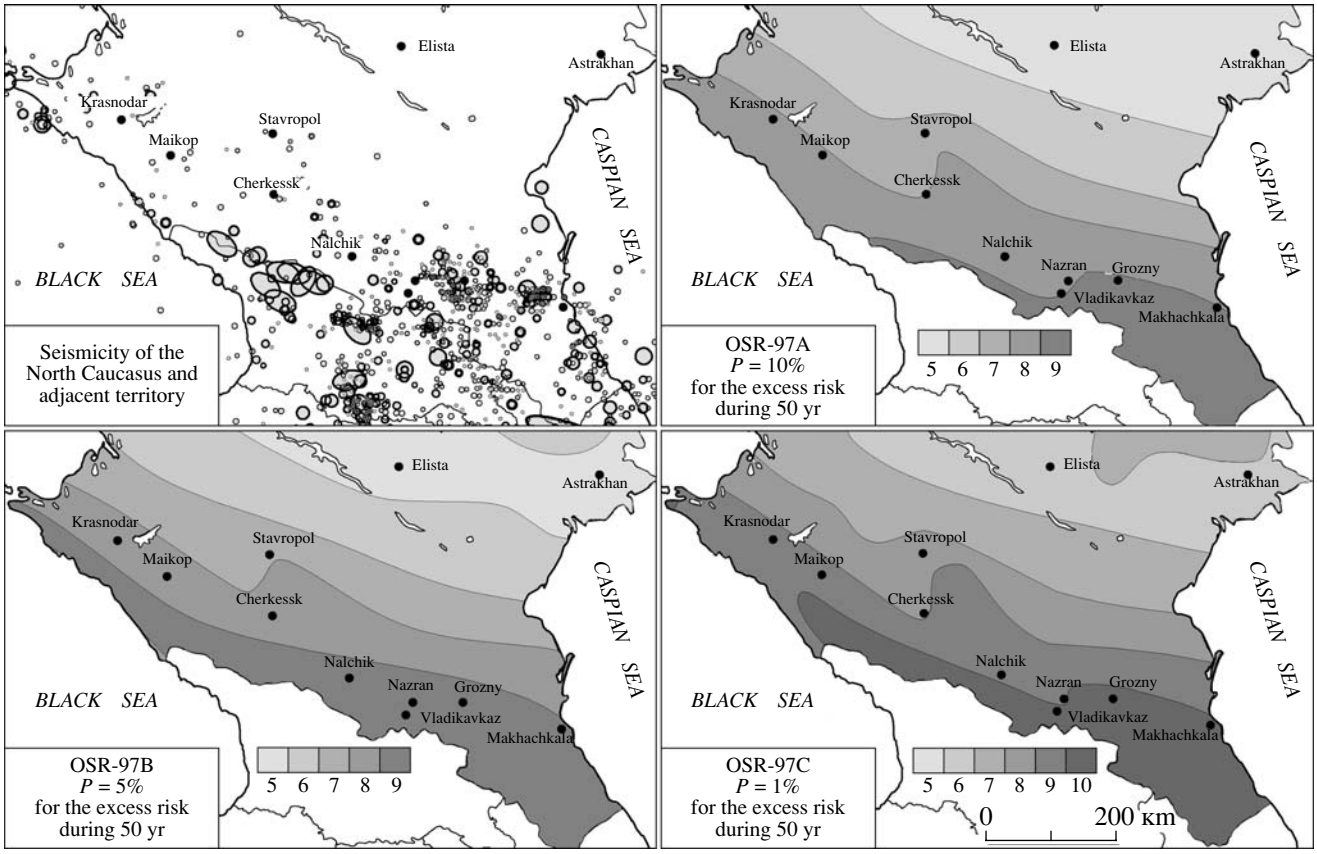

Fig. 1. Seismicity of the Caucasus and fragments of the OSR-97 maps of the general seismic zoning of the Russian Federation. In the seismicity map, the ellipses and circles are, respectively, sources of known earthquakes with $M = 6.8$ and with $M = 6.7$–3.5 that occurred from ancient times through 2005. The OSR-97 (A, B, C) maps show zones with different seismic intensities, within which the seismic effect is allowed to be exceeded during 50-yr intervals at probabilities of 10, 5, and 1%, respectively.

tion (OSR-97), which were constructed at IPE RAS in 1991–1997 and quantify the seismic hazard of the territory in terms of the probability that the calculated seismic intensity (in units of the MSK-64 scale) will be exceeded during 50-yr intervals (10, 5, and 1% in the respective maps A, B, and C) [Ulomov, 1999; Ulomov and Shumilina, 1999].

The eastern North Caucasus, including the territories of Daghestan, Chechnya, Ingushetia, and North Ossetia, is seismically most active. Large seismic events here include the earthquakes of 1830 ($M = 6.3$, $I_0 = 8$–9)[1] and 1970 ($M = 6.6$, $I_0 = 8$–9) in Daghestan and the Chernogorsk earthquake of 1976 ($M = 6.2$, $I_0 = 8$–9) in Chechnya. The Teberda 1905 ($M = 6.4$, $I_0 = 7$) and Chkhaltinsk 1963 ($M = 6.4$, $I_0 = 9$) earthquakes occurred in the western part, near the frontier with Russia. The largest of the known Caucasian earthquakes occurred in Azerbaijan in 1902 (Shemakha, $M = 6.9$, $I_0 = 8$–9), in Armenia in 1988 (Spitak, $M = 6.9$, $I_0 = 10$), and in Georgia in 1991 (Racha-Dzhava, $M = 6.9$, $I_0 = 8$–9) and 1992 (Barisakho, $M = 6.3$, $I_0 = 8$–9). These earthquakes were felt in the territory of Russia as events of an intensity of up to 5–6. On the Scythian plate, adjacent to the North Caucasus, local seismicity is associated with the Stavropol uplift, partially encompassing Adygeya, the Stavropol Territory, and the Krasnodar Territory. The magnitudes of the earthquakes known here have not reached $M = 6.5$ as yet. A strong Lower Kuban earthquake ($M = 6.0$, $I_0 = 7$) occurred in 1879. Historical records yield evidence for a catastrophic Pontic earthquake (63 BC) that destroyed a number of towns on both sides of the Kerch Strait. Numerous strong or perceptible earthquakes have been noted in the areas of Anapa, Novorossisk, and Sochi, as well as in other zones of the Black Sea coast and in the water areas of the Black and Caspian seas. As seen from Fig. 1, the band 200–300 km wide extending all along the state frontier is the most hazardous territory in southern Russia. Seismic shocks with intensities of 8, 9, and 10 are possible here with various degrees of probability. The Black Sea coast is seismically very hazardous, and earthquakes with intensities of 8–9 or higher are possible here.

[1] Henceforward, the magnitude M means the magnitude M_s determined from surface seismic waves and the seismic intensity at the epicenter I_0 is given on the MSK-64 macroseismic scale.

DETECTION OF POTENTIAL EARTHQUAKE SOURCES

The location of PESs and the determination of times of their next activation still remains the most important problem of seismology. An insufficient use of seismogeodynamic models that adequately reflect the structural and dynamic coupling between the geophysical medium and seismic processes is one of the causes of the slow progress in this field of seismological knowledge. However, the study of the structure of local, regional, and global seismicity reveals well-expressed regular patterns in the spatial and energy (magnitude) distributions of earthquake sources that can be used for the location of potential sources and the determination of the maximum magnitudes of earthquakes generated by them.

The method of predominant interepicentral distances (IEDs), based on the study of regular features in distributions of faults of various ranks and sources of earthquakes of various magnitudes [Ulomov, 1987, 1988; Ulomov et al., 1989], is one of methods used for PES detection. It was shown that dimensions (ranks) of faults and distances between them are controlled by thicknesses and strength properties of rock sequences involved in faulting. The thicker the layer cut by faults into blocks, the deeper and longer the faults themselves and the larger the blocks formed by them. On the contrary, with a decrease in the thicknesses of the layer, the dimensions of corresponding faults and related blocks become smaller. It has been shown that the distances δ_j between nodes of intersecting faults and, accordingly, the dimensions of blocks possess a clearly expressed tendency toward grouping in accordance with their ranks, approximately doubling their lateral and vertical dimensions on transition from one rank to another. The discovered ordering induces the corresponding order not only in systems of tectonic faults and geoblocks but also in the hierarchy of earthquake sources: larger earthquakes have sources separated by greater distances. Thus, seismic sources ranked according to the magnitude intervals $M \pm 0.2$ and the radiated elastic energy E are regularly distributed not only in time (the earthquake recurrence law) but also in space (the spacing law of seismic sources) [Ulomov, 1987, 1988, 1993a, 1998].

Intracontinental (intraplate) seismicity studies [Ulomov, 1974; Ulomov et al., 1989] showed that the average statistical distances δ_M (km) or δ_K (km) between neighboring epicenters of the closest pairs of seismic sources with the dimensions (lengths) L_M (km) or L_K (km) located along lineament structures and characterized by the magnitude M or the energy class K depend on M and K through the following relations:

$$L_M = 10^{(0.6M - 2.5)}, \quad L_K = 10^{(0.333K - 3.832)}, \qquad (1)$$

where $K = \log E = 1.8M + 4.0$, and

$$\delta_M = 10^{(0.6M - 1.94)}, \quad \delta_K = 10^{(0.333K - 3.272)}. \qquad (2)$$

As follows from (1) and (2), the quantity $\delta/L \approx 3.63$ does not depend on the magnitude and is invariant under it, thereby reflecting the self-similarity in the hierarchy of dimensions of interacting geoblocks and their earthquake sources.

Dependences (1) and (2) can be expressed more consistently using the earthquake energy classification in the SI system, where E is measured in joules and L_E and δ_E in meters:

$$L_E = 2^{\log E}/\sqrt{3.5}, \quad \delta_E = 2^{\log E}\sqrt{3.5}. \qquad (3)$$

It was also shown that relations (1) correspond to the expression with a clearer physical sense

$$L = \sqrt[3]{2E/\mu\varepsilon^2}, \qquad (4)$$

which relates in the simplest way the energy of deformation E (J) to the crust volume L^3 (m^3) under critical conditions of its fracture, when the strain field ε of the medium is represented only by the shear component μ. The generally accepted average values $\mu = 3.0 \times 10^{10}$ Pa (3×10^{11} dyn/cm^2) and $\varepsilon = 1.45 \times 10^{-4}$ are consistent with dependence (1). Both of these quantities characterize the strength and dynamic properties of the medium and can slightly change from one region to another, which is no less important because an internally consistent system of physical data and relation (1) can serve as a reference point for regional reconstructions. The coefficient 0.6 at the magnitude M also has a profound physical sense because it reflects a change in the source dimension by a factor of $\sqrt[3]{10}$, i.e., by about two times, if the earthquake seismic energy changes by ten times [Ulomov, 1988; Ulomov et al., 1993]. Deviations from this quantity can be in turn used for estimating the specific volume energy density and the dimensions of seismogenerating volumes of the crust and the entire lithosphere. The quantity δ_M is nothing but the average lateral dimension δ_j of geoblocks that are capable of generating earthquakes with the corresponding maximum magnitude M_{max}.

Table 1 presents the average and interval (in parentheses) values obtained with the use of formulas (1) and (2)

Table 1

M	L_M, km	δ_M, km
9.0 (8.8–9.2)	800 (600–1000)	2880 (2200–3800)
8.5 (8.3–8.7)	400 (300–600)	1440 (1100–1900)
8.0 (7.8–8.2)	200 (150–260)	720 (550–950)
7.5 (7.3–7.7)	100 (80–130)	360 (280–480)
7.0 (6.8–7.2)	50 (40–65)	180 (140–240)
6.5 (6.3–6.7)	25 (19–33)	90 (70–120)
6.0 (5.8–6.2)	12 (10–17)	46 (35–60)
5.5 (5.3–5.7)	6 (5–8)	23 (17–30)

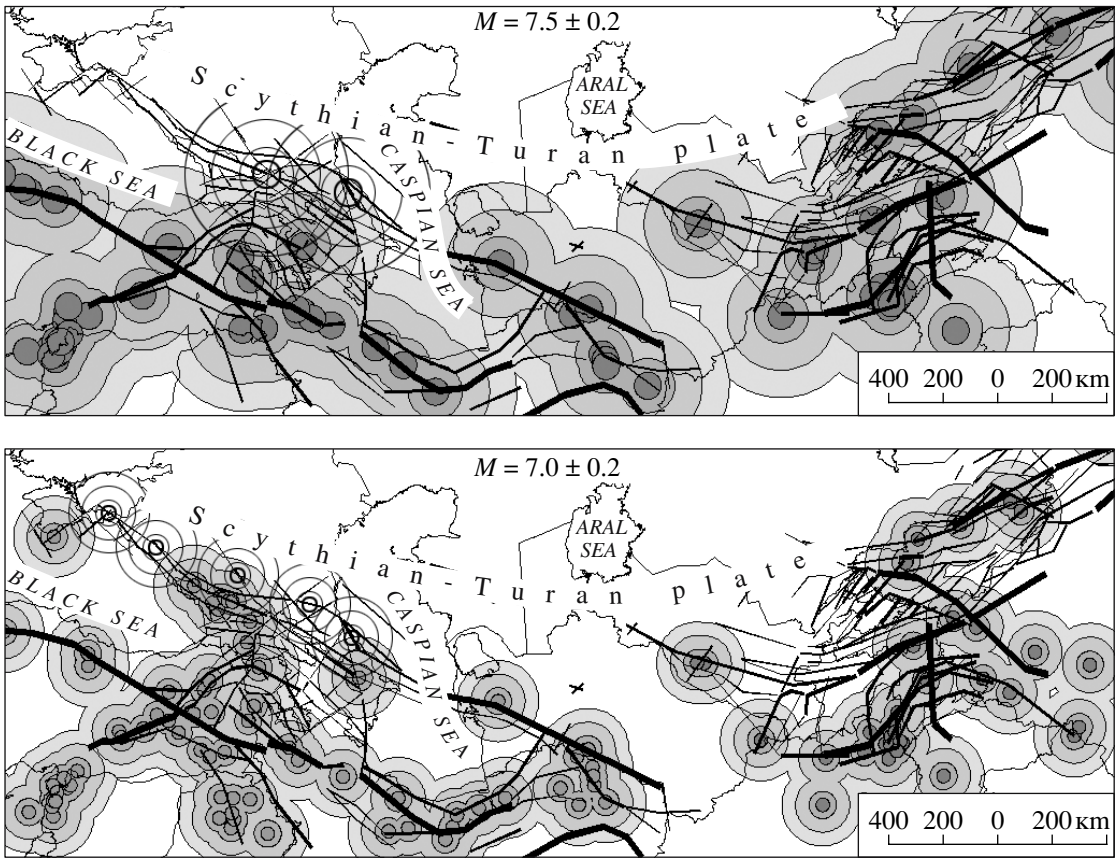

Fig. 2. Clusters of sources of earthquakes in given magnitude intervals in the Iran–Caucasus–Anatolia and Central Asia regions and locations of potential seismic sources in the North Caucasus. Seismic lineaments generating earthquakes with magnitudes of 8.0 ± 0.2 to 6.0 ± 0.2 are shown by lines correspondingly decreasing in thickness.

for the source dimension L_M, predominant IED δ_M, and earthquake magnitude M.

In order to discover PESs with $M = 7.0 \pm 0.2$ and 7.5 ± 0.2 in the North Caucasus, Fig. 2 presents the distributions of epicenters of such earthquakes that occurred at various times in the Alpine Iran–Caucasus–Anatolia and Hercynian Central Asia regions. The thick lines in the maps show all known lineaments that generated earthquakes with magnitudes of 6.0 ± 0.2, 6.5 ± 0.2, 7.0 ± 0.2, 7.5 ± 0.2, and 8.0 ± 0.2 and were used for the construction of the OSR-97 seismic zoning maps [Ulomov and Shumilina, 1999]. The darkest circles show sources of $M = 7.0 \pm 0.2$ and 7.5 ± 0.2 earthquakes having the diameters $L_M = 50$ and 100 km calculated from formulas (1) and (2).

Concentric circles of three diameters corresponding to one, two, and three source dimensions L_M are described around each epicenter. The gray shades of the circles corresponding to different intensities provide a clear idea of the relationships between the dimensions of sources L_M and their IEDs δ_M, as well as of the phenomenon of clusterization, i.e., the degree of overlapping of areas of the corresponding circles at a given magnitude level. Thus, it is easy to reveal (even visually) that, in the Iran–Caucasus–Anatolia region, these areas begin to overlap at epicentral distances that are considerably smaller compared to Central Asia.

We should note that formulas (1) and (2), obtained analytically and empirically for intracontinental regions, describe generalized dependences mainly related to the seismogeodynamics of rather strong geological structures of Hercynian, Caledonian, and older ages [Ulomov, 1974, 1987, 1988]. However, Alpine fold structures have not been considered from this standpoint as yet.

Figure 3 shows the theoretical dependences of δ_M versus magnitude calculated by formulas (1) and (2) and the empirical values obtained for the Central Asia and Iran–Caucasus–Anatolia regions and approximated by the respective formulas

$$\delta_M = 10^{(0.59 - 1.98)}, \quad (5)$$

$$\delta_M = 10^{(0.54M - 1.92)}. \quad (6)$$

The numerical values of these quantities are given in Table 2, presenting also the hypothetical lengths L of seismic sources in the Central Asia and Iran–Caucasus–Anatolia regions, calculated under the assumption of the

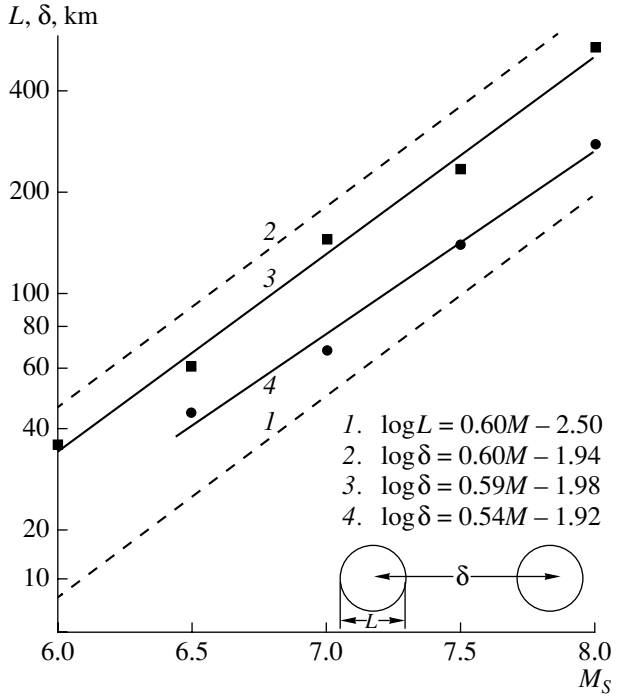

Fig. 3. Dependence of the predominant interepicentral distance δ_M on the magnitude M in the Iran–Caucasus–Anatolia and Central Asia regions: (*1*, *2*) generalized M dependences of the earthquake source length L (*1*) and δ_M (*2*) calculated by formulas (1) and (2) (see the text); (*3, 4*) lines approximating experimental values of interepicentral distances obtained for earthquakes in Central Asia (*3*) and the Iran–Caucasus–Anatolia region (*4*) (the correlation coefficient in both cases is $R2 = 0.99$).

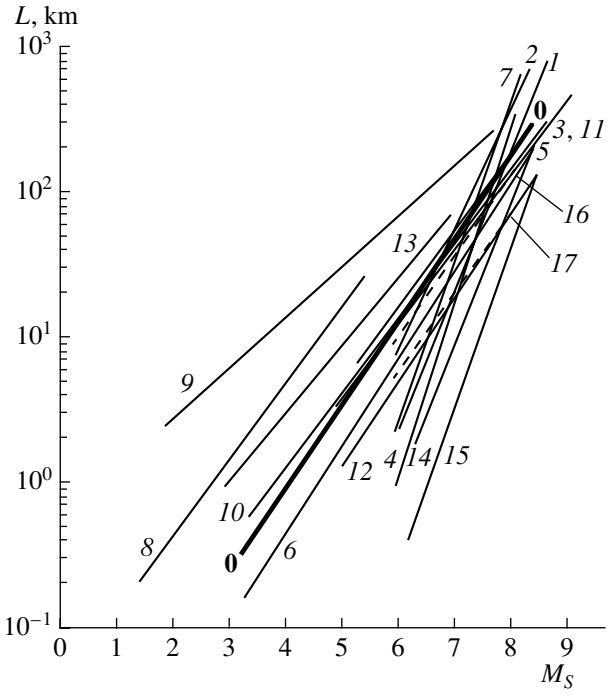

Fig. 4. Dependences of the earthquake source dimension L (km) on the magnitude M_S from data of various authors [Ulomov, 1987, 1988]: (*1*) [Tocher, 1958]; (*2*) [Iida, 1965]; (*3*) [Otsuka, 1964]; (*4*) [Iida, 1959]; (*5*) [Dambara, 1966]; (*6*) [Press, 1967]; (*7*) [Ambraseys and Zatopek, 1968]; (*8*) [Wyss and Brune, 1968]; (*9*) [Bonilla, 1970]; (*10*) [Ulomov, 1971, 1974]; (*11*) [Shebalin, 1971, 1974]; (*12*) [Matsuda, 1975]; (*13*) [Riznichenko, 1976]; (*14*) [Solonenko, 1973]; (*15*) [Khromovskikh, 1977]; (*16*, *17*) the relations $L(M)$ calculated for Central Asia (*16*) and the Iran–Caucasus–Anatolia region (*17*); (**0**) calculated by the formula $\log L = 0.6M - 2.5$.

validity of the generalized relationship $\delta_M/L_M = 3.63$. As seen, these values for the Iran–Caucasus–Anatolia region are nearly twice as small as those for Central Asia and two to three times smaller than the generalized values.

Without going into a more rigorous analysis of the nature of these phenomena, we may suggest that Alpine structures of the Iran–Caucasus–Anatolia region are characterized by a higher specific density of elastic energy released at the same magnitudes in substantially smaller volumes of the medium compared to epiplatform structures of the Tien Shan.

To gain an idea of the diversity of information on the relationships between seismic source dimensions and earthquake magnitudes, the data presented in [Ulomov, 1987, 1988] are summarized in Fig. 4. As seen, with a wide scatter in the $L(M)$ values characteristic of the intervals of small and moderate magnitudes, the closest results are obtained at large magnitudes, which is quite natural because, in this case, the statistics is supplemented by ruptures clearly expressed at the Earth's surface. It is important that dependence (1) averages rea-

Table 2

Regions	Relations	$M = 6.0$	$M = 6.5$	$M = 7.0$	$M = 7.5$	$M = 8.0$
Generalized dependences	$\delta_M = 10^{(0.6M - 1.94)}$	46	91	182	363	724
	$L_M = 10^{(0.6M - 2.5)}$	12.7	25.1	50.1	100	199
Central Asia	$\delta_M = 10^{(0.59 - 1.98)}$	36.3	71.6	141.2	278.6	549.5
	$L(\delta_M)$	10.0	19.7	38.9	76.7	151.4
Iran–Caucasus–Anatolia	$\delta_M = 10^{(0.54M - 1.92)}$	20.9	38.9	72.4	134.9	251.2
	$L(\delta_M)$	5.8	10.7	19.9	37.2	69.2

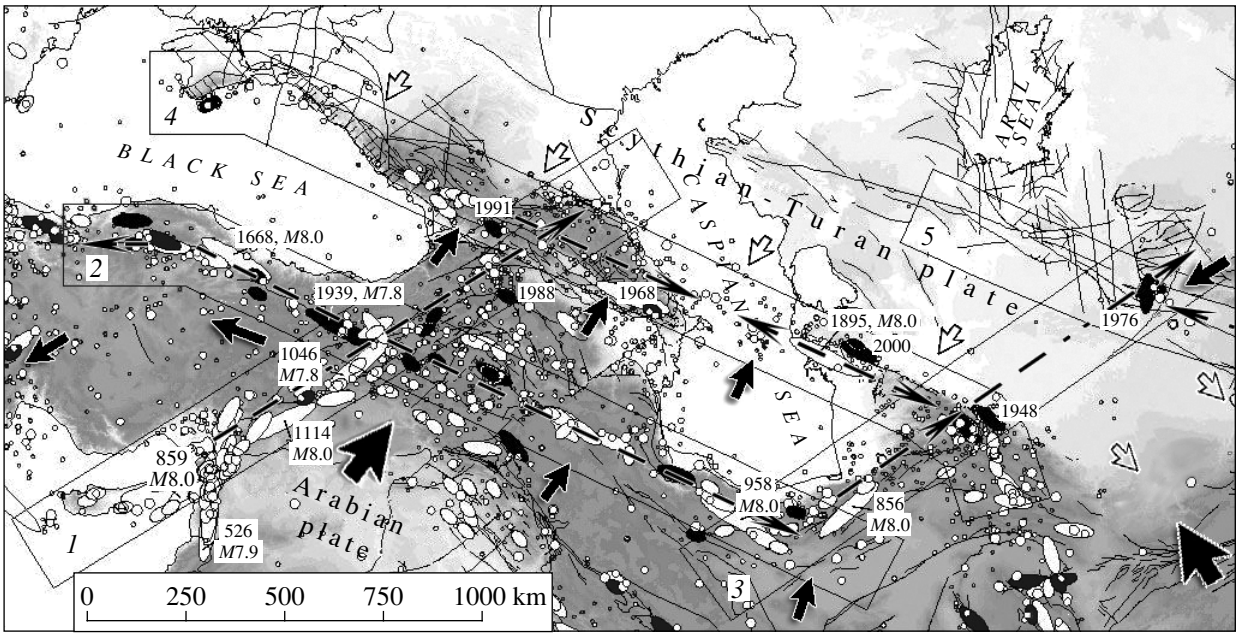

Fig. 5. Locations of the profiles (bands) encompassing seismic lineaments along which the spatial–temporal and energy development of seismogeodynamic processes was studied (a fragment from the figure presented in [Ulomov et al., 2006]). Profiles: (*1*) Cyprus–Caucasus, a length of 1870 km; (*2*) Anatolia–Elburz, 2270 km; (*3*) Elburz–Turan, 1520 km; (*4*) Crimea–Kopet Dagh, 2500 km; (*5*) South Tien Shan, 2520 km. The thick arrows show the directions of geodynamic motions of different structures. The open arrows show the response of the Scythian-Turan platform to the compressive forces produced by the Arabian lithospheric plate (the large arrow) and Alpine structures of the Iran–Caucasus–Anatolia region. The broken arrows show migration directions of seismic activation along the profiles. Earthquake occurrence dates and magnitudes are indicated near some sources. The sources of earthquakes that occurred after 1900 are shown as blackened areas.

sonably well this diversity of relationships. Figure 4 also plots the relationships (shown by the broken lines) we obtained for Central Asia and the Iran–Caucasus–Anatolia region. They lie inside the region covered by the other plots.

The PESs (open circles in Fig. 2) identified in the North Caucasus and Ciscaucasia territories are obtained by the IED method, taking into account the statistical scatter in δ_M values. The potential magnitudes $M = 7.5 \pm 0.2$ and 7.0 ± 0.2 characterize, respectively, two and five of these sources. As in the case of real sources, circles of diameters multiple of the dimension L_M are described around the PESs. These circles help to estimate the probability of the mapped location of PES epicenters because, according to statistical calculations, a circle of a radius three times larger than the source dimension corresponds to a 95% probability that the PES epicenter will lie within this circle.

DEVELOPMENT OF SEISMOGEODYNAMIC PROCESSES

Seismicity of the Cyprus–Caucasus and Crimea–Kopet Dagh Profiles

As noted above, the Cyprus–Caucasus and Crimea–Kopet Dagh lineament structures are the seismically most hazardous in the Russian part of the North Caucasus and Ciscaucasia. In our previous publications [Ulomov et al., 2002, 2005, 2006; Ulomov, 2003, 2004], we showed that the vast majority of lineaments are characterized by a high degree of alignment of seismic sources along them and by clearly expressed processes of seismic activation migration, which allows one to estimate the seismic potentials of such structures and develop methods of long-term prediction of the seismic situation.

The spatial–temporal development of seismogeodynamic processes was examined along profiles encompassing the most structured seismicity and the related lineaments [Ulomov et al., 2006]. Some results of these investigations are presented in Fig. 5, where the earthquake sources are shown in the same way as in Fig. 1 and the lineament structures whose seismogeodynamic regimes were studied are outlined by bands.

As seen from Fig. 5, the Cyprus–Caucasus (*1*) and Elburz–Turan (*3*) profiles extend along the direction of the geodynamic forces exerted by the Arabian plate, whereas the three other profiles, Anatolia–Elburz (*2*), Crimea–Kopet Dagh (*4*), and western South Tien Shan (*5*), extend across their direction. It was also shown that the orientations of lineament structures largely predefine the specific features of their seismogeodynamic development. Long-term prediction of large earthquakes was performed by the analysis of cumulative plots characterizing the accumulation of events with time in terms of their numbers normalized to their magnitude intervals. A comprehensive discussion of the results is given

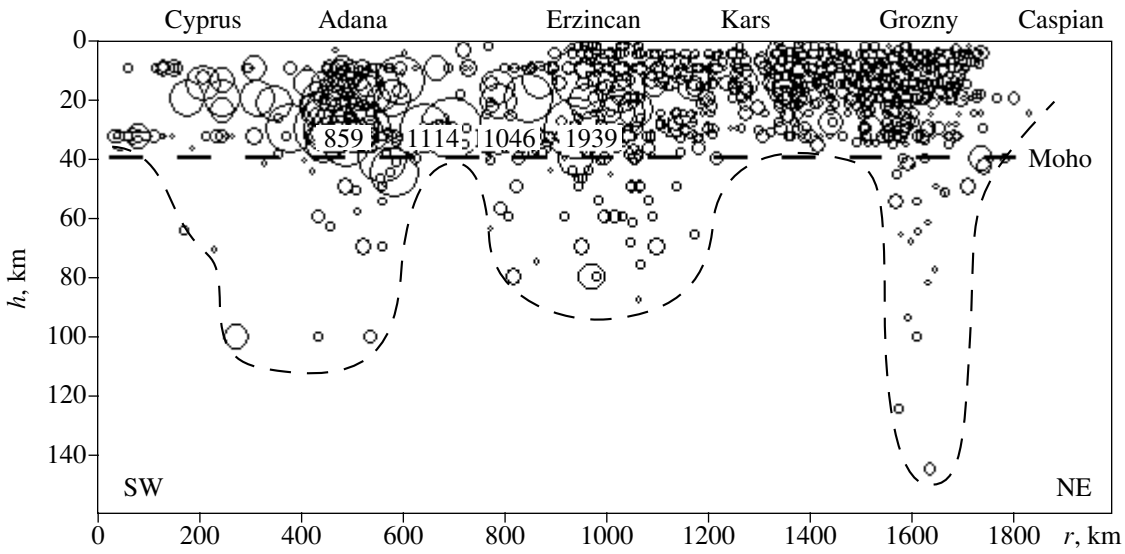

Fig. 6. Depth (h, km) distribution of earthquake hypocenters along the Cyprus–Caucasus profile. The distance r (km) is measured from the SW termination of the profile. Earthquake hypocenters are shown by circles whose diameters increase with magnitudes increasing from $M = 3.5 \pm 0.2$ to 8.0 ± 0.2. The occurrence dates are indicated for the largest seismic events with $M = 8.0 \pm 0.2$ (see also Fig. 5). The Moho boundary is shown tentatively by a horizontal broken line. The thin broken line shows, also tentatively, the lower boundary of deeper earthquake sources.

in [Ulomov et al., 2006]. Below, we present data on large earthquakes that occurred only within the Cyprus–Caucasus and Crimea–Kopet Dagh profiles, most important for long-term prediction of large earthquakes in potential sources located in the south of European Russia.

The Cyprus–Caucasus profile (*1*) is a key profile for estimating the seismic hazard in the North Caucasus and Ciscaucasia. The profile begins on Cyprus, coincides in strike with the East Anatolian fault, and crosses the Caucasus in the NE direction, reaching the Caspian water area. The seismotectonics of this segment of the central part of the Alpine–Himalayan fold belt has been the subject of many studies and has been seismically studied fairly well.

The evidence for large ($M > 7.0 \pm 0.2$) earthquakes in the SW part of the Cyprus–Caucasus profile is available for period longer than 3000 yr (from 1356 BC). Four earthquakes with $M \geq 7.8$ (526, $M = 7.9$; 859, $M = 8.0$; 1046, $M = 7.8$; and 1114, $M = 8.0$) have been revealed here over the historical period (526–1114) but no earthquakes with a magnitude $M \geq 6.8$ occurred here from 1900 to the present.

Large earthquakes with $M = 7.3$ and 7.0 occurred in the central part of the profile in 1872 and 1893, and its NE half was appreciably activated in the period 1900–2004, when numerous earthquakes with $M \geq 6.8$ occurred in 1905, 1924, 1939, 1966, and 1971 in Turkey. The Erzincan 1939 earthquake ($M = 7.8$) was the largest of them. Destructive earthquakes in Armenia (Spitak) and Georgia (Racha-Dzhava) occurred in 1988 and 1991.

An intense release of seismic energy during six centuries (526–1114) followed by an equally long period of relative seismic quiescence (1114–1939) is a characteristic feature of the seismicity along the entire profile under consideration.

All along the profile, the majority of earthquake sources are located in the upper crust (Fig. 6). An insignificant number of weak earthquakes on the Cyprus segment is accounted for solely by their absence in the catalog we used. However, the NE termination of the Cyprus–Caucasus profile is actually characterized by an abrupt seismicity decrease toward the Caspian Sea.

Three areas of deeper hypocenters (down to 100–150 km) are clearly recognizable along the profile. The first area encompasses SW Turkey and Cyprus; the second is the Erzincan area, where this profile intersects with the Anatolia–Elburz profile; and the third is located in the Sunzhenskii trough of the eastern Greater Caucasus.

The possible presence of zones with seismic sources in the upper mantle in the Caucasus and along the entire profile has been widely discussed in the literature [Lebedeva, 1958; Tskhakaya, 1962; Polyakova, 1985; and others]. Our studies showed that the nature of such seismic events is associated with the zone extending from the Kopet Dagh, across the central Caspian Sea and along the Greater Caucasus, up to the Crimea [Ulomov et al., 1999, 2002, 2003; Ulomov, 2003]. Analyzing instrumental data over the period 1911–1958, Lebedeva [1958] identified several earthquakes with sources below the crust, including the earthquake of 1954 in the Sunzhenskii trough with a hypocenter at a depth of about 80 km. Shebalin [1974] and Tskhakaya [1962]

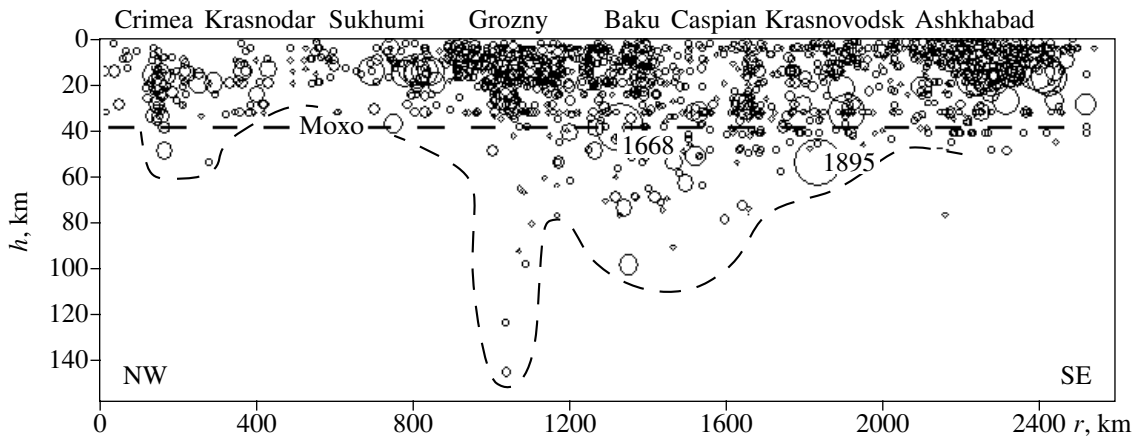

Fig. 7. Depth (h, km) distribution of earthquake hypocenters along the Crimea–Kopet Dagh profile. The distance r (km) is measured from the NW termination of the profile. The legend is the same as in Fig. 6.

also pointed to the presence of sources in the upper mantle of the Caucasus. However, these data were subsequently revised and were classified as intracrustal events in [*New Catalog* …, 1977]. Only the source of the August 10, 1912, earthquake in this edition of the catalog had a depth of 50 km and the magnitude $M = 5.7$. Later, the data on deep sources in the Caucasus, including the area of the Terek-Sunzhenskii trough, were incorporated in a catalog designed for solving OSR-97 problems [*Special Catalogue* …, 1995].

The Crimea–Kopet Dagh profile (*4*) was investigated in detail in [Ulomov et al., 1999, 2002, 2003, 2005; Ulomov, 2003]. Like the Anatolia–Elburz lineament, this profile is transverse to the direction of the geodynamic forces produced by the Arabian plate and includes two offshore areas, the NE Black Sea and the central Caspian Sea. This profile is, on the whole, fairly well constrained by geological, geophysical, and seismological evidence and can be divided into four parts. Its western part extends from the Crimea to the middle of the Greater Caucasus and is characterized by a relatively small number of weak and moderate earthquakes and by paleoseismological evidence for very large ($M \approx 7.0$) ancient seismic events north of Sukhumi (shown by ellipses in Fig. 5). This region also includes the strong ($M = 6.8$) Yalta earthquake of 1927 and seismic events of similar magnitudes such as the Anapa earthquake of 800 BC ($M = 6.5$), the Kerch earthquakes of 63 BC ($M = 6.4$, Ponticapea) and 275 AD ($M = 6.4$), and the Lower Kuban earthquake of 1879 ($M = 6.0$). There is evidence for seismic events of 1100 and 1750 with $M = 7.0 \pm 0.2$ in the NW Greater Caucasus. The Teberda (1905, $M = 6.4$), Chkhaltinsk (1963, $M = 6.4$), and Racha-Dzhava (1991, $M = 6.9$) earthquakes occurred here in areas where such large events were unknown previously. As noted above, the eastern North Caucasus is seismically most active. The third, offshore area is located in the central Caspian Sea, and the fourth area includes the Kopet Dagh and the intersection with the Elburz–Turan profile (*3*).

The largest earthquakes along this profile occurred on both sides of the Caspian Sea: in the Shemakha area in 1668 ($M = 7.8$; the SE offshoots of the Greater Caucasus) and to the south of the city of Krasnovodsk in 1895 ($M = 7.9$; western Turkmenistan). The Kazandzhik 1946 ($M = 7.0$) and Balkhan 2000 ($M = 7.3$) earthquakes occurred here in the 20th century and at the beginning of the 21st century. Earthquakes of 943 ($M = 7.6$), 1209 ($M = 7.4$), 1389 ($M = 7.3$), and 1405 ($M = 7.6$) are known to have occurred over the historical period on the Kopet Dagh segment of the profile. The Gifan (Germab) 1929 ($M = 7.2$) and Ashkhabad 1948 ($M = 7.3$) earthquakes occurred here in the 20th century. The next Shemakha earthquake ($M = 6.9$) occurred in 1902 on the other side of the Caspian Sea. The zone of the Caspian water area connecting the Cheleken and Apsheron peninsulas is seismically active. Earthquakes with $M = 6.0$–6.5 occurred here in 1911, 1931, 1935, 1986, and 1989.

A vertical cross section along the Crimea–Kopet Dagh profile is presented in Fig. 7, whose horizontal and vertical scales and source symbols are the same as in Fig. 6. Similar to the Cyprus–Caucasus profile, the eastern parts of the Greater Caucasus and North Caucasus (the city of Grozny area) are characterized by the deepest sources. A fairly long zone with sources as deep as 100 km is traceable farther to the east, including the water area of the Caspian Sea and its western coast. The crustal base (the Moho boundary) along each of the profiles under consideration (Figs. 6, 7) is shown tentatively as a horizontal dashed line. Like the Earth's surface, the real Moho is not flat. It is shallowest in the southern Caspian Sea [Ulomov et al., 1999, 2002, 2003, 2005; Ulomov, 2003].

Seismic Regimes of Lineaments

The recurrence plots of earthquakes with magnitudes from $M = 4.0 \pm 0.2$ to 8.0 ± 0.2 are presented in Fig. 8 for each profile under consideration. The magni-

tudes in intervals ±0.2 with a step of 0.5 and the decimal logarithms of the average annual number N of corresponding seismic events are plotted on the abscissa and ordinate axes, respectively. The bold dots in the figure show the observed recurrence rate of such earthquakes. The exponential dependences $N(M)$, presented on the logarithmic scale as straight lines, are obtained by approximating the empirical values by the maximum likelihood method. The equations of these lines are presented below each plot in Fig. 8.

As seen, the slope angles b of the approximating lines have quite realistic values, which confirms that the areas of the profiles under consideration were chosen correctly. The length of these profiles is controlled by the length of relict subduction zones associated with the lineaments, and their width is determined by the zone of seismogeodynamic influence of the major faults of a lineament.

It was shown in [Ulomov and Shumilina, 1999] that, in nearly all regions of North Eurasia, large earthquakes occur much more frequently than could be expected from linear extrapolation of the recurrence plots of weak and moderate earthquakes toward larger magnitudes. This circumstance is due to faulting processes in a medium whose density, strength, and dynamic characteristics increase with depth. Thus, large earthquake sources extending to great depths arise under conditions differing from those of shallower smaller sources. However, if the medium were of one type, its fragmentation would obey fractal laws and the logarithmic plots would actually be linear [Ulomov, 1974].

In the case under consideration, this phenomenon is most clearly expressed in the recurrence plot for the Crimea–Kopet Dagh profile, where all empirical points of the numbers of $M > 6.5$ earthquakes lie above the approximating line. Recall that the one-sided deviation of empirical points of the number of large magnitude events from the approximating curve is due to the maximum likelihood method, which, as distinct from the least squares approximation, takes into account the statistics and weights of events. This pattern seems to be invalid for the Cyprus–Caucasus profile. However, underestimated numbers of earthquakes with $M = 7.5 \pm 0.2$ and 8.0 ± 0.2 can be regarded as evidence for a deficit of such seismic events along this profile, which only emphasizes the potential hazard of their occurrence and can be directly related to their prediction in the potential source at the NE termination of the Cyprus–Caucasus lineament.

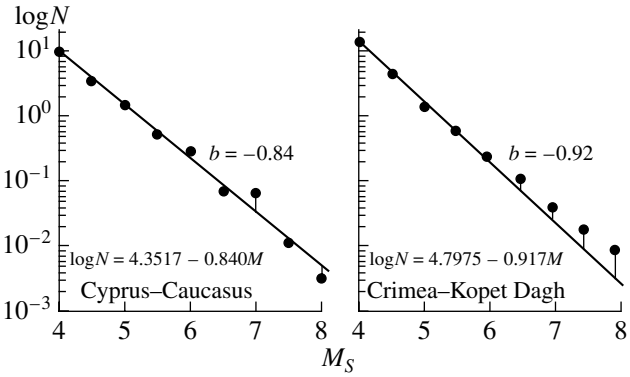

Fig. 8. Earthquake recurrence plots in the magnitude interval $M = 4.0 \pm 0.2$–8.0 ± 0.2 within the Cyprus–Caucasus and Crimea–Kopet Dagh lineaments.

Migration of Seismic Activation

The phenomena of seismic activity migration along each of the five profiles presented in Fig. 5 are discussed in detail in our previous work from the standpoint of the propagation of deformation G-waves (geons) along seismic lineaments, provoking the breakage of cohesion in faults and the occurrence of earthquakes. The migration is unidirectional and most pronounced on profiles coinciding in orientation with respect to acting forces, whereas it has different directions on transverse profiles. The Cyprus–Caucasus profile belongs to the former, and the Crimea–Kopet Dagh profile, to the latter [Ulomov et al., 2006].

The spatial–temporal distribution of seismic sources with $M = 7.0 \pm 0.2$, 7.5 ± 0.2, and 8.0 ± 0.2 that arose along the Cyprus–Caucasus profile beginning from 1820 is presented in the upper panel in Fig. 9. The distances measured from the SW termination of this profile are plotted on the abscissa axis, and the occurrence times (years) of seismic events within this profile are plotted on the ordinate axis. The shaded circles of different diameters mark the occurrence times of all known earthquakes with the specified magnitudes. The thin arrows connect events in accordance with their occurrence succession, and the thick dashed arrow shows the generalized direction of the migration of seismic sources at a velocity of about $V = 5$ km/yr within a deformation wave about 400 km in length λ, bounded in the figure by parallel dashed lines. The thick arrow is actually the traveltime curve of the deformation G-wave.

The migration processes along the transverse Crimea–Kopet Dagh profile are less ordered and are not considered here. These phenomena are rather comprehensively analyzed in [Ulomov et al., 2006], where other uncertainties in the ideas of seismicity along this profile are also noted. For example, the evidence on the Shemakha earthquake of 1668 ($M = 7.8$) is hypothetical in many aspects and is not acknowledged by all seismologists. The evidence on the triple earthquake of 1100 ($M = 7.0$) is also doubtful. Only the southeasterly trend toward the Kazandzhik earthquake of 1946 ($M = 7.0$) and a relatively recent earthquake with $M = 7.3$ in the offshoots of the Greater Balkhan in western Turkmenistan can be discussed with some certainty. It is also possible that the Ashkhabad earthquake of 1948 and other, close in time, seismic events that occurred in its vicinity are associated with the Krasnovodsk earthquake of 1895.

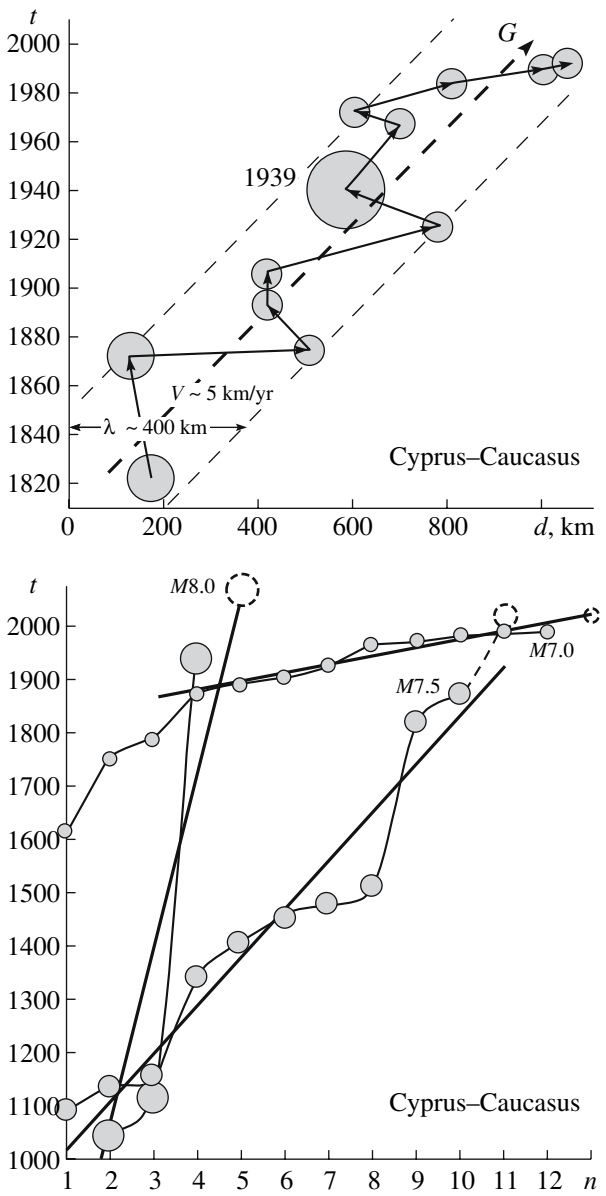

Fig. 9. Migration of the seismic activation (the upper panel) and the occurrence succession of seismic events in the magnitude intervals $M = 7.0 \pm 0.2$, 7.5 ± 0.2, and 8.0 ± 0.2 along the Cyprus–Caucasus profile. The circles of small, medium, and large diameters correspond to these intervals of magnitudes.

The source of the Yalta earthquake of 1927 ($M = 6.8$), located at the western termination of the profile, is fairly isolated.

The knowledge of the velocity V of the G-wave is favorable for long-term prediction of earthquakes in a given magnitude interval and their most probable occurrence areas.

It is noteworthy that a distinct (especially after the earthquake of 1939) migration of the entire set of sources of earthquakes with magnitudes under consideration has taken place in the NW direction along the Cyprus–Caucasus profile during about 250 yr. The two last earthquakes with $M = 7.0 \pm 0.2$ occurred in Armenia (Spitak, 1988) and Georgia (Racha-Dzhava, 1991). The hazard of further migration in the same direction remains.

Earthquake Occurrence Succession

The gradual accumulation of seismic events in the given magnitude intervals on the Cyprus–Caucasus profile and their prediction for the future are illustrated in the lower panel in Fig. 9. By analogy with ordinary traveltime curves of seismic waves, the time (years) is plotted on the ordinate axis of this plot and the ordinal numbers of earthquakes in each chronological sequence, on the abscissa axis. The straight lines approximate the entire set of events with the corresponding magnitudes, and the curves are obtained by the spline interpolation of the initial data set. The slopes of the straight lines determine the average recurrence intervals of earthquakes with the given magnitudes in each sequence of events. The shaded circles indicate earthquakes that have already occurred, and the open circles indicate predicted earthquakes whose occurrence times are calculated through the extrapolation of the approximating lines or splines.

If seismic events occurred uniformly in time, all of them would be located strictly on straight lines, thereby facilitating prediction of the occurrence times of subsequent earthquakes. Although the real pattern is not so ideal, it is nevertheless characterized by clearly expressed regular features. With decreasing slope of the approximating line (or its segment), the accumulation rate of events (their recurrence rate) increases and, accordingly, the recurrence interval becomes shorter. On the contrary, steeper segments correspond to a slower rate and a rarer occurrence of earthquakes. Therefore, the plots steepen with a magnitude increase and flatten with a decrease. A wavelike configuration is inherent in virtually all spline curves and evidently reflects the contemporary general geodynamics of the entire Iran–Caucasus–Anatolia region and its individual parts. Thus, an increase in the recurrence rate of earthquakes is followed by their rarer occurrence and, sometimes, by a long period of seismic quiescence.

The vertical axis intercepts of the plots are another noteworthy circumstance. Thus, while the slope angles of the plots adequately reflect the average long-term (short-term in the case of curves) recurrence intervals of earthquakes of the corresponding magnitudes, the absolute level of the event accumulation plots on the time axis is somewhat artificial because it depends on the choice of representative initial data and thereby on the degree of completeness of the earthquake catalogs used. This is clearly seen from the plot for $M = 7.0 \pm 0.2$, constructed for the time interval (beginning from 1874) whose seismic representativeness is more reliable. An anomalous drop in the plot in the interval 1616–1874 is evidence for the incompleteness of this part of the

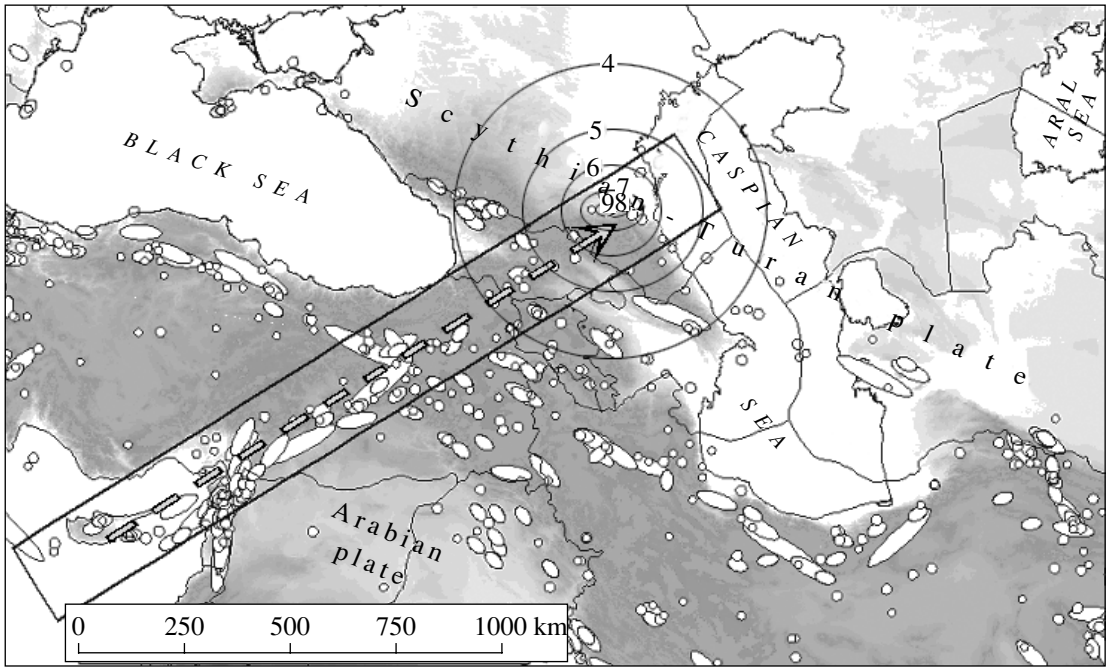

Fig. 10. The expected seismic effect of a potential source of $M = 7.0$ earthquakes in the eastern North Caucasus.

earthquake catalog. The extrapolation of this plot to the next ordinal number of such earthquakes points to a 20-yr prognostic interval (from 2013 to 2036) of the most probable occurrence of an earthquake with the magnitude $M = 7.0 \pm 0.2$ along this profile.

Analyzing further the process of accumulation of seismic events along the Cyprus–Caucasus profile, attention should be given to the 133-yr absence of earthquakes with $M = 7.5 \pm 0.2$ in this area. The last of such earthquakes occurred in 1872 in southern Turkey. The occurrence probability of a next earthquake is fairly high. Neither can one rule out a longer period of seismic quiescence similar to that existing between 1513 and 1824 after earthquakes with $M = 7.5 \pm 0.2$ that often occurred before this time interval.

Presently, it is difficult to say something definite about prediction of seismic events with $M = 8.0 \pm 0.2$ along the profile under consideration. The Erzincan earthquake of 1939 was the last of such events. As seen, after the two similar earthquakes of 1046 ($M = 7.8$) and 1114 ($M = 8.0$), such events were not observed in SE Turkey over more than 800 yr.

Evidently, the predictions of earthquakes in the considered magnitude intervals relate to the entire area of the Cyprus–Caucasus profile. If the seismic migration and the inferred positions of potential sources are taken into account, one can draw more definite conclusions on concrete places and expectation time of predicted earthquakes.

Prediction of the Seismic Effect

The expected seismic effect of an $M = 7.0$ PES in the eastern North Caucasus is illustrated in Fig. 10. The sources of the known earthquakes with magnitudes from 6.0 ± 0.2 to 8.0 ± 0.2 are shown here with the use of the same legend as in the preceding maps. The Cyprus–Caucasus profile is shown as an elongated rectangle, and the broken line ending with an arrow indicates the direction of the seismic activation migration along the profile over the past 200 yr. The calculated (model) isoseismal lines of the seismic effect are presented in an idealized form as concentric circles.

As seen from Fig. 10, the seismic effect in the epicentral area can attain an intensity of 9. Earth tremors of an intensity of 3–4 will be felt throughout the Caucasus, and tremors of an intensity of 3 or less, far beyond the Caucasus, in the Crimea, in northern Iran, and in the west of Turkey and Turkmenistan. It cannot be ruled out that such an event will occur, as mentioned above, in the time interval from 2013 to 2036. It is also probable that its occurrence place will lie within the inferred PES (Fig. 10).

As regards the recurrence interval T of earthquakes with the magnitude $M_{max} = 7.0$ within this potential source, it can be determined on the basis of "individual" recurrence plots constructed for the area of the circle with the radius $R = \delta_{M\,max}/2$ described around the PES epicenter. The value of T_{max} is determined from the number of seismic events with different magnitudes $M < M_{max}$ corresponding to one "individual" event with M_{max} [Ulomov, 1987, 1988]. We constructed such plots with the use of both generalized formula (2) and for-

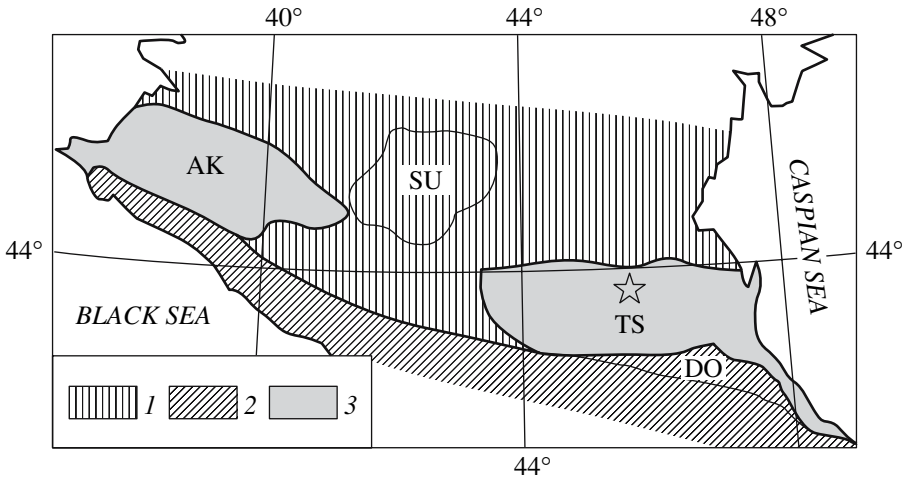

Fig. 11. Tectonic scheme of North Ciscaucasia (modified after [Mikhailov et al., 1999]): (*1*) epi-Paleozoic Scythian platform; (*2*) mountainous structures of the Greater Caucasus; (*3*) contemporary Azov-Kuban (AK) and Terek-Sunzhenskii (TS) foredeeps; SU, Stavropol uplift; DO, Daghestan overthrust. The star is the epicenter (43.76°N, 45.68°E) of the $M = 5.1$ earthquake of October 12, 2006, which occurred within the Terek-Sunzhenskii trough, 50 km north of the city of Grozny, and had a source depth of 145 km (data of the RAS Geophysical Service).

mula (5) for the inferred value of δ_M (see Table 2). In the first case, the circle radius was set equal to $R = 100$ km and the resulting recurrence interval of earthquakes with $M_{max} = 7.0$ was $T \approx 400$ yr. In the second case, at $R = 40$ km, the recurrence interval decreased to $T \approx 350$ yr, which is due to the fact that the North Caucasus belongs to the Iran–Caucasus–Anatolia region. As noted above, no evidence is available as yet on earthquakes of such a magnitude in this region.

DISCUSSION

The locations of the main structural elements of the North Caucasus and Ciscaucasia are shown in Fig. 11, which is taken, with some simplifications, from [Mikhailov et al., 1999], analyzing the deep geodynamic mechanism of the formation of foredeeps, including those of North Ciscaucasia.

The Terek-Sunzhenskii trough, which is located in its eastern part and is the main subject of our investigations, has a complex structure, as distinct from the Azov-Kuban trough, whose geological structure is simple. The crustal structure of the Terek-Sunzhenskii trough has not been studied sufficiently well on the basis of deep seismic sounding and gravity data and the available geological evidence. On the other hand, precisely this region is characterized by the deepest sources of earthquakes. Whatever the notions about this site (a subduction zone relict [Ulomov, 1993a] or a result of upper mantle convection [Mikhailov et al., 1999]), the eastern parts of North Ciscaucasia and the Greater Caucasus with its Daghestan overthrust are anomalous. As shown in Fig. 6, very large earthquakes with magnitudes of up to $M = 8.0 \pm 0.2$ have already occurred in two of the three anomalous areas of this type characterized by deep seismic sources.

It is also noteworthy that a certain activation of seismic processes in this region has recently been observed. The $M = 5.1$ earthquake of October 12, 2006, within the Terek-Sunzhenskii trough, 50 km north of the city of Grozny, is the latest example of this activation. Its epicenter is marked by the star in Fig. 11. Its large hypocentral depth (about 150 km) points to the geodynamic activation of a fairly thick seismically active layer, which in turn can indicate a high magnitude of a potential earthquake. According to data of the RAS Geophysical Service (Obninsk), a few weak earthquakes with deep sources were recorded in the Terek-Sunzhenskii trough over the period from 2000 through October 2006.

The reconstructions performed in this study on the basis of the method of predominant interepicentral distances between sources of large earthquakes of the Iran–Caucasus–Anatolia region also indicate that the seismic hazard in this area of the North Caucasus is real. The study of specific features characteristic of the development of seismogeodynamic processes along the Cyprus–Caucasus profile showed that, at a high probability, the next earthquake with $M = 7.0 \pm 0.2$ can occur between 2013 and 2036 and cause intensity-9 tremors in the epicentral area. It is quite probable that such an earthquake will occur before this period. A similar time interval can be accepted for the activation of one of the two potential sources of earthquakes with $M = 7.5 \pm 0.2$, whose seismic effect can be considerably stronger. The occurrence probability of such an earthquake is also rather high because, with an average 85-yr recurrence interval of such events along the Cyprus–Caucasus profile, they have been absent here for 134 yr. It is conceiv-

able that this earthquake will also occur at the NE termination of the profile.

Our investigations will be continued and extended to the Black Sea coast of the Greater Caucasus and Ciscaucasia, where objects of national significance, such as the largest health resorts and the Rostov nuclear power plant, are located. Likewise, the interrelations between regional and global geodynamics will be further studied.

ACKNOWLEDGMENTS

This work was supported by the Russian Foundation for Basic Research, project no. 04-05-64912, and by the program of the Presidium of the RAS "Environmental and Climatic Changes: Natural Catastrophes and Related Anthropogenic Catastrophes," direction 1: "Seismic Processes and Catastrophes."

REFERENCES

1. N. N. Ambraseys, "Some Characteristic Features of the Anatolian Fault Zone," Tectonophysics, No. 2/3, 143–165 (1970).
2. N. N. Ambraseys, "Studies in Historical Seismicity and Tectonics," Earthquake Inform. Bull. **12** (1) (1980).
3. N. N. Ambraseys and A. Zatopek, "The Varto Ustukran (Anatolia) Earthquake of 19 August 1966," Bull. Seismol. Soc. Am. **58** (1), 47–102 (1968).
4. M. G. Bonilla, "Surface Faulting and Related Effects," in *Earthquake Engineering*, Ed. by R. L. Weigel (Prentice-Hall, New Jersey, 1970).
5. T. Dambara, "Vertical Movements of the Earth's Crust in Relation to the Matsushire Earthquake," J. Yead Soc. Japan, No. 12, 18–45 (1966).
6. K. Iida, "Earthquake Energy and Earthquake Fault," J. Earth Sci. Nagoya Univ. No. 7, 98–107 (1959).
7. K. Iida, "Earthquake Magnitude, Earthquake Fault and Source Dimensions," J. Earth Sci. Nagoya Univ. No. 13, 115–132 (1965).
8. V. S. Khromovskikh, "Correlation of Parameters of Coseismic Deformations with the Magnitude and Intensity," in *New Catalog of Strong Earthquakes in the USSR* (Nauka, Moscow, 1977) [in Russian].
9. T. M. Lebedeva, "Earthquakes with Subcrustal Sources in the Caucasus, Tr. IG AN Gruz. SSR **17**, 139–159 (1958).
10. T. Matsuda, "Magnitude and Recurrence Interval of Earthquake from a Fault," Zisin, J. Seismol. Soc. Japan, No. 28, 269–283 (1975).
11. V. O. Mikhailov, E. P. Timoshkina, and R. Polino, "Foredeep Basins: The Main Features and Model of Formation," Tectonophysics **308**, 345–360 (1999).
12. *New Catalog of Strong Earthquakes in the USSR* (Nauka, Moscow, 1977) [in Russian].
13. M. Otsuka, "Earthquake Magnitude and Surface Fault Formation," J. Phys. Earth, No. 12, 19–24 (1964).
14. M. Otsuka, "Earthquake Magnitude and Surface Fault Formation," Zisin, J. Seismol. Soc. Japan **18** (1), 1–8 (1965).
15. T. P. Polyakova, *Seismicity of the Central Mediterranean Belt* (Nauka, Moscow, 1985) [in Russian].
16. F. Press, "Dimensions of the Source Region for Small Shallow Earthquakes," in *VESIAC Conf. Report 7885-1-X* (1967), pp. 155–163.
17. Yu. V. Riznichenko, "Source Dimensions of a Crustal Earthquakes and the Seismic Moment," in *Investigations on Physics of Earthquakes* (Nauka, Moscow, 1976), pp. 9–27 [in Russian].
18. N. V. Shebalin, "Estimation of Dimensions and Position of the Tashkent Earthquake Source from Macroseismic and Instrumental Data," in *Tashkent Earthquakes of 1966* (FAN, Tashkent, 1971), pp. 68–79 [in Russian].
19. N. V. Shebalin, *Strong Earthquake Sources in the USSR* (Nauka, Moscow, 1974) [in Russian].
20. V. P. Solonenko, "Paleoseismology," Izv. Akad. Nauk SSSR, Fiz. Zemli, No. 9, 3–16 (1973).
21. *Special Catalogue of Earthquakes of the Northern Eurasia (SCENE)*, Ed. by N. V. Kondorskaya and V.I. Ulomov (1995); http://socrates.wdcb.ru/scetac/ and http://www.seismo.ethz.ch/gshap/neurasia/nordasiacat.txt
22. D. Tocher, "Earthquake Energy and Ground Breakage," Bull. Seismol. Soc. Am., No. 48, 147–153 (1958).
23. A. D. Tskhakaya, "On Depths of Caucasian Earthquakes," Izv. Akad. Nauk SSSR, Ser. Geofiz., No. 5, 577–584 (1962).
24. V. I. Ulomov, "Rock Deformation in the Source Area of the Tashkent, April 26, 1966, Earthquake," Izv. Akad. Nauk SSSR, Fiz. Zemli, No. 9, 22–30 (1971).
25. V. I. Ulomov, *Dynamics of the Central Asia Crust and Earthquake Prediction* (FAN, Tashkent, 1974) [in Russian].
26. V. I. Ulomov, "On the Dimension Relations between Sources and Nucleation Regions of Earthquakes," Dokl. Akad. Nauk Uzb. SSR, No. 9, 39–40 (1987).
27. V. I. Ulomov, "Source Seismicity and Long-Term Prediction of Earthquakes," in *Seismological Problems of Central Asia* (FAN, Tashkent, 1988), pp. 32–87 [in Russian].
28. V. I. Ulomov, "Global Ordering of Seismogeodynamic Structures and Some Aspects of Seismic Zoning and Long-Term Prediction of Earthquakes," in *Seismicity and Seismic Zoning of Northern Eurasia* (OIFZ RAN, Moscow, 1993a), Vol. 1, pp. 24–44 [in Russian].
29. V. I. Ulomov, "Waves of Seismogeodynamic Activation and Long-Term Prediction of Earthquakes," Fiz. Zemli, No. 4, 43–53 (1993b).
30. V. I. Ulomov, "Focal Zones of Earthquakes Modeled in Terms of the Lattice Regularization," Fiz. Zemli, No. 9, 20–38 (1998) [Izvestiya, Phys. Solid Earth **34**, 717–733 (1998)].
31. V. I. Ulomov, "Seismogeodynamics and Seismic Zoning of Northern Eurasia," Vulkanol. Seismol., Nos. 4–5, 6–22 (1999).
32. V. I. Ulomov, "A Three-Dimensional Model of the Lithosphere Dynamics, Seismicity Structure, and Variations in the Caspian Sea Level," Fiz. Zemli, No. 5, 5–17 (2003) [Izvestiya, Phys. Solid Earth **39**, 353–364 (2003)].
33. V. I. Ulomov, "Implication of Horizontal Tectonic Movements for Seismogeodynamics and Seismic Hazard Pre-

diction," Fiz. Zemli, No. 9, 14–30 (2004) [Izvestiya, Phys. Solid Earth **40**, 710–724 (2004).

34. V. I. Ulomov, R. P. Fadina, and A. R. Yarmukhamedov, *Probability Density of the Position of Earthquake Sources in Uzbekistan. Geological and Geophysical Investigations of Seismically Hazardous Zones* (Ilim, Frunze, 1989) [in Russian].
35. V. I. Ulomov, T. P. Polyakova, L. S. Shumilina, et al., "Experience of Mapping Earthquake Sources," in *Seismicity and Seismic Zoning of Northern Eurasia* (OIFZ RAN, Moscow, 1993), Vol. 1, pp. 99–108 [in Russian].
36. V. I. Ulomov and L. S. Shumilina, *A Set of Maps (1 : 8000000) of General Seismic Zoning of the Russian Federation (OSR-97). Explanatory Note and the List of Cities and Inhabited Localities in Seismically Hazardous Regions* (OIFZ, Moscow, 1999) [in Russian].
37. V. I. Ulomov, T. P. Polyakova, and N. S. Medvedeva, "Seismogeodynamics of the Caspian Sea Region," Fiz. Zemli, No. 12, 76–82 (1999) [Izvestiya, Phys. Solid Earth **35**, 1036–1042 (1999)].
38. V. I. Ulomov, T. P. Polyakova, and N. S. Medvedeva, "On the Long-Term Prediction of Strong Earthquakes in Central Asia and the Black Sea-Caspian Region," Fiz. Zemli, No. 4, 31–47 (2002) [Izvestiya, Phys. Solid Earth **38**, 276–290 (2002)].
39. V. I. Ulomov, M. Mokhtari, T. P. Polyakova, and N. S. Medvedeva, "Geodynamic Origin of Variations of Seismic Regime of Caspian Area and Level of Caspian Sea," in *Abstracts of 4th Int. Conf. on Seismology and Earthquake Engineering. SEE4. 12–14 May, 2003* (Tehran, 2003), p. 33.
40. V. I. Ulomov, I. P. Kuzin, O. N. Solov'eva et al., "Seismogeodynamic Migration Processes in the Central Caspian Sea and Adjacent Structures of the Caucasus and Kopet Dagh," Fiz. Zemli, No. 2, 13–22 (2005) [Izvestiya, Phys. Solid Earth **41**, 104–113 (2005)].
41. V. I. Ulomov, T. I. Danilova, N. S. Medvedeva, and T. P. Polyakova, "Seismogeodynamics of Lineament Structures in the Mountainous Regions Bordering the Scythian-Turan Plate," Fiz. Zemli, No. 7, 17–33 (2006) [Izvestiya, Phys. Solid Earth **43**, 551–566 (2006)].
42. M. Wyss and J. N. Brune, "Seismic Moment, Stress and Source Dimensions for Earthquakes in California–Nevada Region," J. Geophys. Res. **73**, 4681–4694 (1968).